

Nearest-neighbor Ising antiferromagnet on the fcc lattice: Evidence for multicritical behavior

S. Kämmerer, B. Dünweg, K. Binder, and M. d'Onorio de Meo

Institut für Physik, Johannes Gutenberg-Universität Mainz, Staudingerweg 7, Postfach 3980, D-55099 Mainz, Germany

(Received 12 June 1995)

The phase behavior of the Ising model with nearest-neighbor antiferromagnetic interactions on the fcc lattice in a homogeneous magnetic field is studied by means of large-scale Monte Carlo simulations. In accordance with the most recent of the previous investigations, but with significantly higher accuracy, it is found that the “triple” point at which the disordered phase coexists with both the AB phase as well as with the A_3B phase (corresponding to the model's lattice gas interpretation as a binary alloy A_xB_{1-x} , such as $\text{Cu}_x\text{Au}_{1-x}$) occurs at a *nonzero* temperature. However, there is numerical evidence that the first-order jumps on the three associated phase coexistence lines tend to *zero* when approaching this point, which means that it is, in fact, a *multicritical* point. Since the Landau theory does not support this picture, and the simulation data do not definitely exclude a usual triple point with small jumps, the question about the nature of the point must be considered as unresolved.

I. INTRODUCTION: HAMILTONIAN, GROUND STATES, ORDERED PHASES

More than fifty years after its first mean-field treatment by Shockley,¹ the phase behavior of the Ising model on the face-centered-cubic (fcc) lattice with antiferromagnetic nearest-neighbor interactions in a homogeneous magnetic field still remains a challenge for statistical physics. Compared to “usual” Ising models for antiferromagnetic ordering (or, equivalently, lattice gas models for superstructure formation of binary alloys, see, e. g., Ref. 2), this Hamiltonian,

$$\mathcal{H} = J \sum_{\langle ij \rangle} S_i S_j - H \sum_i S_i \quad (1.1)$$

(where $\langle ij \rangle$ indicates nearest neighbors, $J > 0$ is the exchange coupling, H is the magnetic field, and $S_i = \pm 1$ denotes an Ising spin on site i) has some unusual properties that make phase diagram calculations in the (H, T) (field-temperature) plane particularly difficult. In what follows only $H \geq 0$ will be considered, since the phase diagram is symmetric around $H = 0$.

It is impossible to assign spins to a nearest-neighbor tetrahedron such that all six bonds are antiferromagnetic, i.e., the model exhibits geometrical frustration, resulting in a lack of three-dimensional long-range order at $T = 0$.³ While for $H > 12J$ the ground state is trivially ordered ($S_i = 1$), it is only two dimensionally ordered for $H < 12J$. For $H < 4J$, the ground state is some arbitrary sequence of perfectly antiferromagnetically ordered (100) planes. Since there are two configurations possible per plane, a $4 \times L^3$ system exhibits a ground-state degeneracy of 3×2^{2L} , i.e., a vanishing ground-state entropy per spin in the thermodynamic limit. For $4J < H < 12J$ the ground state is a sequence of (100) planes, which are alternately ferromagnetically ($S_i = +1$) and antiferromagnetically ordered. Again, for each antiferromagnetic plane there are two possible configurations, resulting in a ground-state degeneracy of 6×2^L .

At finite temperature, however, the system exhibits “order out of disorder.” This is an interesting effect of frustration

and has been shown to occur via the exact solution of certain two-dimensional models.^{4,5} In the present system the same phenomenon leads to three-dimensional long-range order for nonzero temperatures, as has been shown via careful analysis of low-temperature series expansions.⁶⁻⁹ It is most easily understood by viewing the many ground states as corresponding to a large number of thermodynamic phases, which coexist at $T = 0$. For each of these phases, the free energy per site f may be calculated by a low-temperature expansion. As a result, one finds that only a small number of phases has minimum free energy per site (these phases admit most low-energy excitations; however, for $H < 4J$ the effect is not seen before the third order). Hence, only those entropically stabilized phases survive in the thermodynamic limit: From Ref. 6 one concludes that the free-energy difference per site (compared to the minimum value) depends on the periodicity of the structure and may be as small as $A(T)/L$, where $A(T) > 0$ is some constant that tends to zero as $T \rightarrow 0$ because of the vanishing Boltzmann weight of the corresponding excitation. Hence, a “pessimistic” estimate of the statistical weight of all the “nondominant” phases is $\exp\{BL - 4L^3\beta(f_{\min} + A/L)\}$ where $\exp(BL) > 1$ estimates the number of phases, and $\beta = 1/(k_B T)$. For sufficiently large L , this is small compared to $\exp\{-4L^3\beta f_{\min}\}$, the statistical weight of the “dominant” ordered phases. However, this consideration also shows that in a Monte Carlo (MC) simulation one needs *unusually large* systems in order to observe the correct asymptotic behavior, and that the effect gets worse with *decreasing* temperature because of the proximity of the phase transition to the less ordered phase at $T = 0$.

The ordered phases, which are singled out by this mechanism, are commonly denoted by AB ($H < 4J$) and A_3B ($4J < H < 12J$), motivated by the “alloy language” in which $S_i = +1$ corresponds to an A atom and $S_i = -1$ to a B atom. A physical example is the Cu-Au system.¹⁰⁻¹⁵ Subdividing the fcc lattice into four interpenetrating simple cubic sublattices (a, b, c, d), the AB ground state is given by two sublattices occupied with $S_i = +1$ and the other two with $S_i = -1$. Since these sublattices can be chosen arbitrarily, this phase is sixfold degenerate. Similarly, the A_3B ground

state is given by one sublattice with $S_i = -1$, while the other three are occupied with $S_i = +1$ (fourfold degeneracy). Since any sublattice permutation can be induced by geometrical symmetry operations, it is obvious that these symmetries also pertain to $T > 0$. More precisely, the phases are defined via their symmetry as follows: In both the AB phase as well as the A_3B phase there exist *two* values for the sublattice magnetization. While in the AB phase two sublattices have the higher magnetization value and the remaining two sublattices the lower one, the A_3B phase is described by three sublattices with identical (high) magnetization, the remaining sublattice having the lower magnetization.

The so-called L' phase, which has been found as a stable phase of the present system in the study by Finel and Ducastelle,¹⁶ applying the tetrahedron-octahedron approximation of Kikuchi's cluster variation method (CVM),^{17,18} has even lower symmetry: In this case there are *three* sublattice magnetization values, one of which is shared by two sublattices. This phase is hence twelvefold degenerate. In the ideal state, these two sublattices have magnetization $m = +1$ and the other two $m = -1$ and $m = 0$ (i.e., random spin orientation), respectively. While this state is a ground-state at $H = 4J$, giving rise to a lower bound on the ground-state entropy per spin,³ the stability of this phase in a finite region of the phase diagram is somewhat controversial. Based on our simulation results, we believe that it is probably an artifact of the CVM (see below).

Even lower symmetry would be obtained if *all four* sublattices had different magnetizations. Such a phase would be 24-fold degenerate; however, this case has never been reported as a stable phase and is not found in the present study either.

A more convenient description of the ordering is obtained as follows: Starting from the four sublattice magnetizations m_a, m_b, m_c , and m_d (varying between -1 and $+1$), we introduce the linearly transformed variables

$$\begin{aligned}\psi_0 &= (m_a + m_b + m_c + m_d)/4, \\ \psi_1 &= (m_a + m_b - m_c - m_d)/4, \\ \psi_2 &= (m_a - m_b + m_c - m_d)/4, \\ \psi_3 &= (-m_a + m_b + m_c - m_d)/4.\end{aligned}\quad (1.2)$$

While ψ_0 is simply the total magnetization, ψ_1, ψ_2 , and ψ_3 are the components of the three-dimensional order parameter $\vec{\psi}$: In the disordered phase all sublattice magnetizations are the same, and hence $\vec{\psi} = (0,0,0)$. The AB phase corresponds to the six vectors $\vec{\psi} = (\pm\psi_{AB}, 0, 0), (0, \pm\psi_{AB}, 0)$, and $(0, 0, \pm\psi_{AB})$. This is the symmetry of the Heisenberg model with cubic anisotropy, for which a first-order transition has been predicted by renormalization-group analysis.¹⁹ Hence, the transition line separating the AB phase from the disordered phase should be of first order.

Similarly, the A_3B phase is described by the four vectors $\vec{\psi} = (\psi_{A_3B}, \psi_{A_3B}, \psi_{A_3B}), (\psi_{A_3B}, -\psi_{A_3B}, -\psi_{A_3B}), (-\psi_{A_3B}, \psi_{A_3B}, -\psi_{A_3B})$, and $(-\psi_{A_3B}, -\psi_{A_3B}, \psi_{A_3B})$, located on the corners of a regular tetrahedron, corresponding to the $q = 4$ state Potts model.²⁰ Therefore, a first-order tran-

sition is also predicted between A_3B and the disordered phase — in three spatial dimensions the Potts model exhibits a first-order transition for $q \geq 3$.²¹ The same conclusion holds for the transition $AB \leftrightarrow A_3B$, since it behaves like a $q = 3$ state Potts model.²⁰ Starting from the, say, $(1/2, 1/2, 1/2)$ state in A_3B (i.e., $m_a = m_b = m_c = 1, m_d = -1$), *one* sublattice must be flipped in order to reach AB . Hence, the three states $(1,0,0), (0,1,0)$, and $(0,0,1)$ can be reached. As in the $q = 3$ state Potts model, these states are located on the corners of a regular triangle.

II. THE CONTROVERSY ABOUT THE PHASE DIAGRAM

The phase behavior of the system is still a matter of debate. The problem has mainly been attacked, with ever-increasing sophistication, by either mean-field-like CVM calculations or MC simulations. Shockley's Bragg-Williams (BW) treatment¹ yielded a phase diagram in which, apart from the disordered phase, only AB, A_3B , and B_3A are present. There is no direct transition from AB to the disordered phase; instead, the system is predicted to first go through the A_3B (or B_3A) phase and then enter the disordered phase—except for $H = 0$, where a direct second-order transition to the disordered phase occurs; hence $H_t = 0, k_B T_t = 4J$ is the location of a multicritical point at which all four phases coexist. Higher orders of the CVM, i.e., the tetrahedron approximation (T-CVM) (Ref. 18) and the tetrahedron-octahedron approximation (TO-CVM) (Ref. 22), found the same phases but a different topology of the phase diagram: Here a triple point occurs at some nontrivial location ($H_t \approx 3J, k_B T_t \approx 1.6J$ for T-CVM, and $H_t \approx 3.5J, k_B T_t \approx 1.2J$ for TO-CVM). These results were refined by the study of Finel and Ducastelle,¹⁶ who located the triple point in T-CVM and TO-CVM at practically the same point ($H_t \approx 3J, k_B T_t \approx 1.5J$). Moreover, these authors found a stable L' phase at low temperatures between the AB and A_3B phases. This phase occurs not only in TO-CVM but also in the lower approximations [T-CVM and even BW (Ref. 23)]. This possibility had been overlooked in the previous studies—the equations had been simplified by *requiring* a certain minimum symmetry.

However, from the MC studies there has been only rather weak evidence for this phase. The results presented in Ref. 24, which is the only simulation that claims to have observed the L' phase, are probably severely hampered by insufficient equilibration times near the phase transitions. As outlined below, our present simulation does not support L' phase stability. Unfortunately, a resolution of the question by means of low-temperature expansions^{6–8} is not possible: The temperature region of validity of the low-temperature series shrinks to zero when one approaches the “superdegenerate” point $H = 4J, T = 0$. Hence, there is no rigorous analysis available by which one could rule out a phase diagram in which the H region of stable L' phase contracts to the single point $H = 4J$ when decreasing T down to zero.

The TO-CVM result was further improved by a “mixed” approach in which an even larger cluster was used in the disordered phase.²⁵ This calculation located the triple point at a significantly lower temperature ($k_B T_t \approx 1.0J$). It is therefore not clear how this result would change when increasing the cluster size even further.

The MC simulations first yielded a very different scenario: Based on data obtained from systems of up to $L=16$,^{26–28} one of the present authors suggested 15 years ago that the triple point actually occurs at $H=4J$, $T=0$ such that the disordered phase separates AB and A_3B for all temperatures $T>0$. This scenario is not ruled out by the rigorous approach either, for the same reason as outlined above. However, the later MC simulations^{9,29–32} found a triple point at $k_B T_t \approx 1.0J$ (as does the present study). Lebowitz, Phani, and Styer⁹ made use of the fact that the large ground-state degeneracy is lifted as soon as the Hamiltonian includes a ferromagnetic next-nearest-neighbor interaction $J_{NNN}<0$, which stabilizes the phases AB and A_3B down to $T=0$. They simulated the system for various J_{NNN} and extrapolated the triple-point temperature to $J_{NNN}=0$, finding $k_B T_t \approx 1.0J$. However, it is not obvious that $T_t(J_{NNN})$ would continue to behave linearly when approaching the degenerate case $J_{NNN}=0$ very closely. The other MC studies^{9,29–32} worked at $J_{NNN}=0$ (as does the present investigation), and emphasized the importance of the occurrence of antiphase boundaries (APB's) because of the degenerate ground states, as discussed above. In particular, it is extremely difficult to observe three-dimensional long-range order in a reasonably long run. Diep *et al.*³² tried to overcome this difficulty by studying the Edwards-Anderson order parameter appropriate for spin-glass order. All these studies, however, worked with system sizes that, from the perspective of the computer power available today, must be considered as rather small, in particular since finite-size effects are unusually important in the present system: Aside from the effects of degenerate ground states and APB's, there is the additional complication of very *weak* first-order transitions in the vicinity of the triple point. This behavior has already been observed in the CVM studies, and probably explains why the CVM runs into particularly severe troubles in that region of the phase diagram: Close to a weak first-order transition one expects a finite but very large correlation length exceeding the cluster size, causing the approximation to break down. Based on the results of the present study, we actually believe that the first-order character *vanishes* at the “triple point,” which, hence, is a *multi-critical* point (see below).

III. MONTE CARLO SIMULATION RESULTS

We employed a standard single spin-flip Metropolis algorithm on $N=4 \times L^3$ lattices with periodic boundary conditions. The program was vectorized by a four-sublattice checkerboard decomposition and obtained 3.1×10^6 spin-flip trials per second on one Cray YMP processor.

The first test runs using an $L=16$ system at $H=0$, $k_B T=1.7J$ showed that a system initialized with a random spin configuration would not order and not even slowly relax into a three dimensionally ordered state, although the state point is well within the AB phase, rather far away from $T=0$, and the system was observed for 10^6 Monte Carlo steps (MCS's, one MCS being defined as a full sweep through the lattice). Instead, the system remained stable in some configuration with APB's. We attempted to circumvent the problem in a similar way as Diep *et al.*;³² however, we did not look at the Edwards-Anderson order parameter but rather at a two-dimensional order parameter: For each (100)

plane perpendicular to the x axis, the staggered magnetization is measured separately and summed up in a root-mean-square sense. This is also done for the y and z directions, and finally the order parameter is obtained as the maximum over the directions. Indeed, such an order parameter is a good indication for a state deep in the ordered phases, and, in principle, its distribution could be used for a finite-size scaling approach to first-order phase transitions.³³ However, it turned out that near the phase boundaries the distribution is extremely broad without exhibiting a well-defined two-peak structure, which is a necessary condition for these methods to work. This is easily understandable, since now there are only $2L^2$ spins in a plane instead of $4L^3$ spins in the bulk available for averaging, resulting in an enormous broadening. Moreover, one should not trust results for such a small system anyway, regardless of the type of order-parameter definition: The occurrence and stability of the APB's clearly shows that an $L=16$ system does not yet behave asymptotically, and hence the phase stability near the superdegenerate point $H=4J$, $T=0$ might well be severely affected by finite-size effects, even including two-dimensional ordering. We, hence, studied larger lattices and performed the above-mentioned test for $L=32$ and 64 . While the $L=32$ system is still somewhat hampered by APB's, the $L=64$ system showed a reasonable tendency towards three-dimensional ordering. We therefore believe that $L=64$ is the *smallest* size for which acceptable results can be expected for the present system, and mere limitations of computer resources prevented us from studying an even larger one.

In this system we carefully searched for a stable disordered and a stable L' phase at low temperatures: For many field values H in the vicinity of $H=4J$ we looked at the time development of the sublattice magnetizations after initializing the system in (a) a random configuration of spins and (b) a configuration with two sublattices occupied with $S_i = +1$, one sublattice with $S_i = -1$ and one sublattice randomly occupied. In all cases, we observed a rather quick development of a three dimensionally ordered state belonging to either the AB or the A_3B phase. These results, therefore, rule out both the existence of a stable L' phase as well as a triple point at $T=0$.

The topology of the phase diagram thus being clarified, we mapped out the phase boundaries. For such a large system we found a finite-size scaling analysis rather hard, because of long equilibration times to sample the full configuration space. Instead we pursued the same approach as in Refs. 26–28 and sampled averages both in the stable as well as the metastable state to obtain hysteresis loops, using not too long runs and relying on the self-averaging property of magnetization ψ_0 , internal energy $U = \langle \mathcal{H} \rangle$, etc. We then calculated branches of the free energy F of the system by thermodynamic integration along suitable paths in the phase diagram and found the location of the first-order transitions at the intersection point of these branches. In particular, we used the relations $N\psi_0 = -\partial F / \partial H$ for integrations along paths parallel to the H axis, and $U = -T^2 \partial(F/T) / \partial T$ for integrations parallel to the T -axis, starting at state points where the free energy is trivially known, i.e., the ground state or the $T=\infty$ state. Data were usually obtained from runs of 10 000 MCS's after discarding 2500 MCS's. Near the triple point we ran the system for 30 000 MCS's after discarding

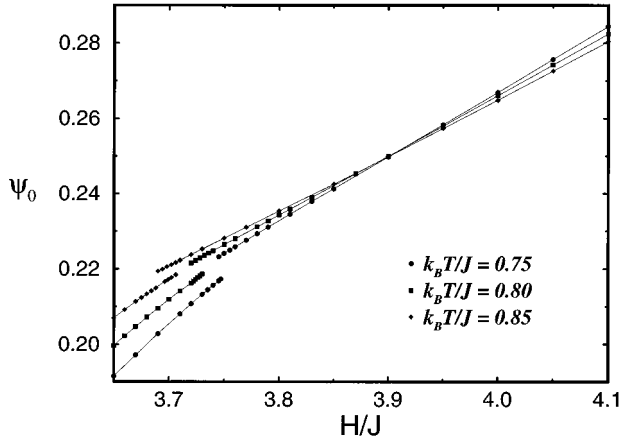


FIG. 1. Total magnetization ψ_0 as a function of magnetic field H , for different temperatures T as indicated in the figure. Hysteresis loops indicate the first-order nature of the transition $AB \leftrightarrow A_3B$.

5000 MCS's. The integral values were then found by fitting cubic splines to the MC data, while the error in the free energies could be easily estimated using standard error propagation: After the usual MC error analysis^{34,35} we used the fact that the data for each state point are statistically independent from each other and that they enter the integral linearly (however, for simplicity we assumed integration according to the trapezoidal rule).

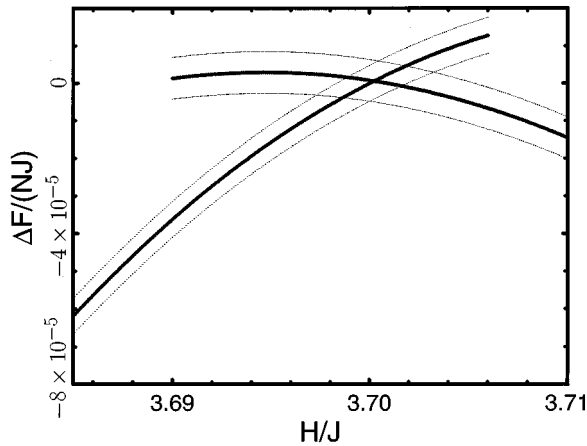


FIG. 2. Branches of the free energy per lattice site in units of the nearest-neighbor coupling $F/(NJ)$, corresponding to the AB phase and the A_3B phase, at temperature $k_B T/J = 0.85$, as a function of magnetic field H . These branches were obtained from thermodynamic integration of the internal energy along paths parallel to the temperature axis (not shown here), and of the magnetization along a path parallel to the field axis (cf. Fig. 1). The free energies (thick lines) result from a cubic spline fit to the data, while the error bars (thin lines) were estimated from standard error propagation of the errors of the individual data points. This allows an estimation of the critical field with well-controlled accuracy, $H_c/J \approx 3.70 \pm 0.003$. The first-order jump of the magnetization corresponds to a nonzero angle between the two branches, which is, however, so small that it would be invisible in a simple plot of F vs H . Hence, we rather show a function $\Delta F/(NJ) = F/(NJ) + 0.22(H/J) + 1.316044$, in order to make the two branches visible and to demonstrate the smallness in free-energy differences.

This procedure is illustrated in Figs. 1 and 2: Figure 1 shows hysteresis loops in $\psi_0(H)$ for three temperatures rather close to the triple point, for the transition $AB \leftrightarrow A_3B$. For the highest temperature, Fig. 2 shows the corresponding intersection of the free-energy branches. It turns out that upon approaching the triple point, the magnetization jump, i.e., the slope difference between the branches, becomes very small, resulting in considerable difficulty to locate the transition field accurately. It is hence very important to have reasonable control over the statistical errors in F , as indicated in Fig. 2.

Similarly to ψ_0 , the other quantities also exhibit very small first-order jumps when approaching the triple point, on all three transition lines. In particular, this is true for the internal energy whose jump can be used for locating the transition temperature along a line of constant field. On all three lines, we hence found that the free-energy intersection method works well only sufficiently far away from the triple point. Close to it, the error in the critical field or temperature, as obtained from plots similar to Fig. 2, is larger than the width of the hysteresis loop, which then is used for a direct rough estimate of the location of the transition. Of course, in this case one has to study a quantity that is rather different in the coexisting phases, i.e., the order parameter. Although this method did not work in the immediate vicinity of the triple point either, because of small first-order jumps and large fluctuations, we were able to get at least somewhat closer, as demonstrated in Fig. 3, where the hysteresis in one order-parameter component (ψ_3) as a function of field is shown for three temperatures rather close to the triple point, again for the transition $AB \leftrightarrow A_3B$.

The resulting phase diagram is shown in Figs. 4 (H - T plane) and 5 (ψ_0 - T plane), respectively. The different meth-

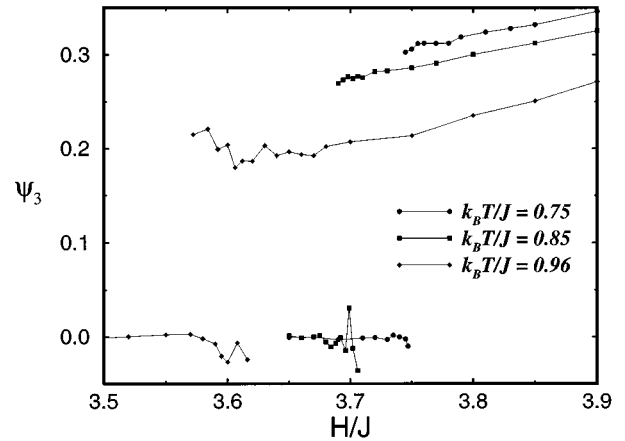


FIG. 3. Hysteresis loop of the order parameter component ψ_3 as a function of magnetic field H , at the transition $AB \leftrightarrow A_3B$, for various temperatures as indicated in the figure. The coordinate system in the three-dimensional order-parameter space (see text) was chosen such that the AB state is described by a vector $\vec{\psi} = (\psi_{AB}, 0, 0)$ with $\psi_{AB} > 0$, while the A_3B state corresponds to a vector $\vec{\psi} = (\psi_{A_3B}, \psi_{A_3B}, \psi_{A_3B})$ with $\psi_{A_3B} > 0$ (cf. text). The scatter in the data (in particular the nonzero values of ψ_3 in the AB phase), observed at the higher temperatures, is because of statistical inaccuracy, indicative of increased sampling problems (slow dynamics and small free-energy barriers between the phases) when approaching the triple (or multicritical) point.

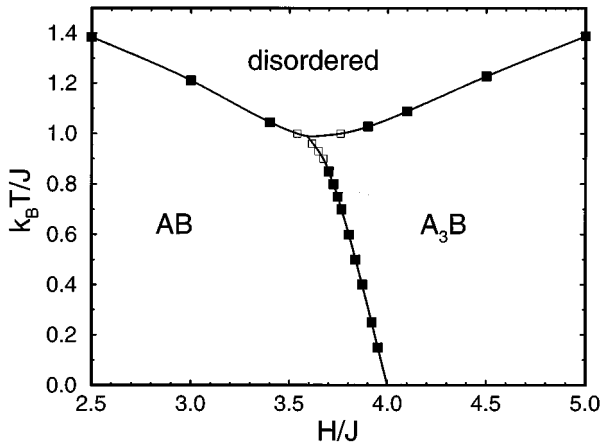


FIG. 4. The phase diagram in the field-temperature plane. The critical fields or temperatures were obtained by thermodynamic integration where possible (filled symbols, cf. Fig. 2) and otherwise by direct inspection of the order-parameter hysteresis loops (open symbols, cf. Fig. 3). The errors are always smaller than the symbol size. All transition lines are of first order. The lines connecting the data points are guides to the eye only.

ods of locating the transition (free-energy intersection vs direct inspection of order parameter hysteresis) are indicated. Altogether, we locate the triple point at $k_B T_t/J = 0.98 \pm 0.02$ and $H_t/J = 3.60 \pm 0.04$. These values are well consistent with the previous studies but distinctly more accurate. As discussed above, all three phase-transition lines should be first order, because of symmetry. The only possible scenario apart from a standard triple point (with small but finite first-order jumps) is a multicritical point: In this case all the jumps would tend to *zero* upon approaching the point. However, our numerical resolution is not sufficient to answer this question unambiguously. Nevertheless, we have tried to check if our order parameter data are consistent with tricritical scaling, $\psi \propto |T - T_t|^{1/4}$, where ψ is the order parameter of the ordered phase along the first-order transition line. This is done in Fig. 6 for the transition $AB \leftrightarrow A_3B$, where the order-

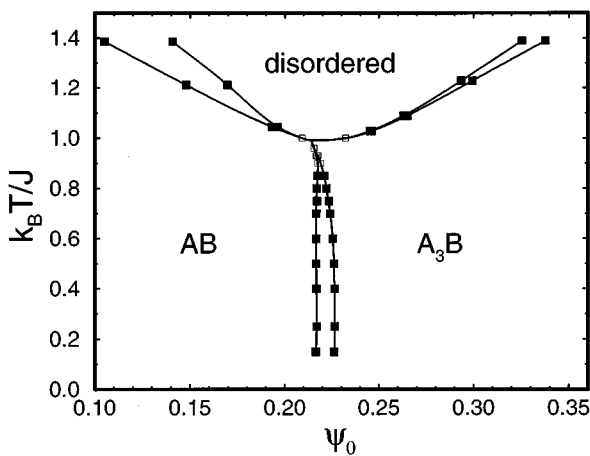


FIG. 5. The phase diagram in the magnetization-temperature plane. The first-order lines of Fig. 4 correspond to two-phase regions, which become extremely narrow when approaching the triple (or multicritical) point. For the meaning of closed and open symbols, see Fig. 4.

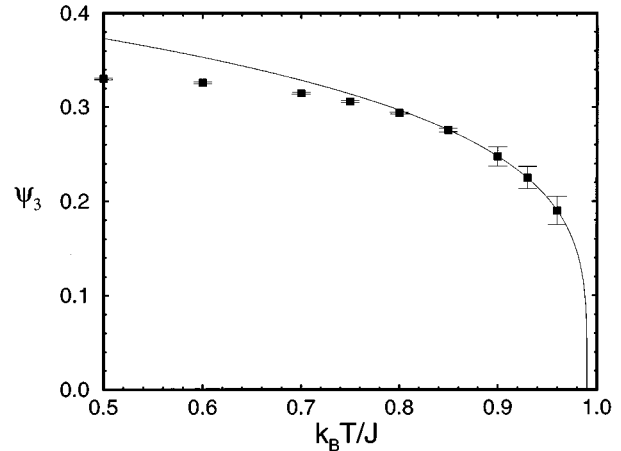


FIG. 6. Order-parameter component ψ_3 of the A_3B phase, along the phase coexistence line with the AB phase, as a function of temperature. For definition of the order parameter $\vec{\psi}$ and choice of the coordinate system in $\vec{\psi}$ space, see text and Fig. 3. The squares represent the Monte Carlo data, while the line is given by the equation $\psi_3 = 0.443436 (0.99 - k_B T/J)^{0.2416}$. Here, the triple temperature $k_B T_t/J = 0.99$ was chosen “by hand” in order to obtain an exponent close to $1/4$. The other two parameters were then obtained by a linear least-squares fit.

parameter component ψ_3 (which is nonzero only in the A_3B phase) is plotted vs temperature (for the other two lines we do not have enough data to make such a comparison meaningful). As shown in the figure, the data are well consistent with tricritical behavior. However, it should be pointed out that this plot proves neither that the order parameter actually tends to zero when $T \rightarrow T_t$ (it might remain finite, as it should for a standard triple point), nor that the exponent is $1/4$ if ψ should actually tend to zero: Depending on the value of T_t , we were able to fit exponents in the range $0.2, \dots, 0.3$.

IV. LANDAU THEORY

It is worthwhile to discuss the existence of a multicritical point analytically also. As will become clear below, Landau theory does *not* support this scenario but rather predicts either a standard triple point or a multicritical point at $H=0$, at which all *four* phases coexist (as in Shockley’s mean-field phase diagram¹). After outlining the theory, we briefly specu-

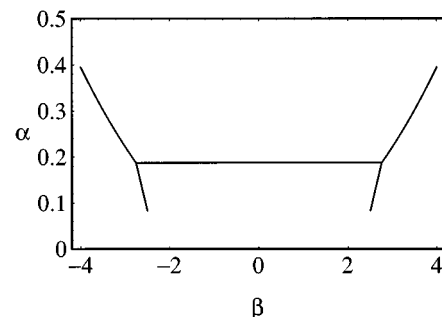


FIG. 7. The phase diagram of the Landau theory in the α - β plane for $\gamma = -1$, $\delta = 2$, and $\nu = 1$ (see text). In this case, the phase diagram exhibits two symmetrical standard triple points.

late about its validity and possible refinements.

In order to find the expression for the Landau free energy, we first wrote down the free energy as a function of the sublattice magnetizations within the mean-field (BW) approximation, transformed this to order parameters [Eq. (1.2)], and expanded up to sixth order in $\vec{\psi}$. From this one obtains the invariant polynomials in $\vec{\psi}$ and the Landau free energy:

$$F = \frac{\alpha}{2} \vec{\psi}^2 - \frac{\beta}{3} \prod_i \psi_i + \frac{\gamma}{4} (\vec{\psi}^2)^2 + \frac{\delta}{4} \left[(\vec{\psi}^2)^2 - \sum_i \psi_i^4 \right] + \frac{\mu}{5} \vec{\psi}^2 \prod_i \psi_i + \frac{\nu}{6} (\vec{\psi}^2)^3 + \frac{\sigma}{6} \left[(\vec{\psi}^2)^3 - \sum_i \psi_i^6 \right] + \frac{\tau}{6} \prod_i \psi_i^2. \quad (4.1)$$

α is a temperaturelike variable, while β can be varied via the field H . All other coefficients are considered constants, and we study the phase diagram of the system in the (α, β) plane.

For the AB phase, we evaluate F on the line $\vec{\psi} = (\psi_{AB}, 0, 0)$, resulting in

$$F_{AB} = \frac{\alpha}{2} \psi_{AB}^2 + \frac{\gamma}{4} \psi_{AB}^4 + \frac{\nu}{6} \psi_{AB}^6, \quad (4.2)$$

where, of course, $\nu > 0$. A first-order transition from AB to the disordered phase (free energy 0) can only occur if $\gamma < 0$. In this case one easily shows that the condition for phase coexistence is $\alpha = (3\gamma^2)/(16\nu)$, since then the free energy simplifies to

$$F_{AB} = \frac{1}{96\nu} \psi_{AB}^2 (4\nu\psi_{AB}^2 + 3\gamma)^2. \quad (4.3)$$

If this first-order line would exhibit a tricritical point, one would need $\gamma = 0$ at that point. We will henceforth concentrate on the case of small (positive or negative) values of γ , and, in particular, assume $3\gamma + 2\delta > 0$. The coefficient δ must be positive, since this term is responsible for the stabilization of the AB phase: $[(\vec{\psi}^2)^2 - \sum_i \psi_i^4]$ is positive for all $\vec{\psi}$ and vanishes only on the (100) axes.

For the A_3B and B_3A phases, we evaluate F along $\vec{\psi} = (\psi_{A_3B}, \psi_{A_3B}, \psi_{A_3B})$:

$$F_{A_3B} = \frac{3}{2} \alpha \psi_{A_3B}^2 - \frac{\beta}{3} \psi_{A_3B}^3 + \frac{3}{4} (3\gamma + 2\delta) \psi_{A_3B}^4. \quad (4.4)$$

The fifth- and sixth-order terms have been omitted, since Eq. (4.4) is already sufficient to describe the phases. For $\beta > 0$, positive values of ψ_{A_3B} are stabilized, corresponding to the A_3B phase, while $\beta < 0$ stabilizes negative ψ_{A_3B} values, i.e., the B_3A phase. Along the line $\alpha = (2\beta^2)/[81(3\gamma + 2\delta)]$ the free energy simplifies to

$$F_{A_3B} = \frac{1}{108(3\gamma + 2\delta)} \psi_{A_3B}^2 (9(3\gamma + 2\delta) \psi_{A_3B} - 2\beta)^2, \quad (4.5)$$

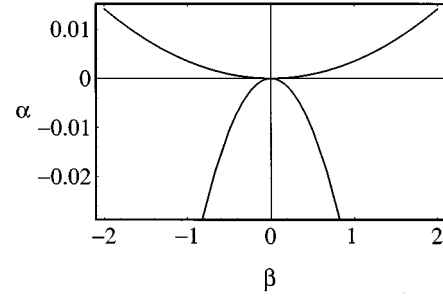


FIG. 8. Same as Fig. 7 but for $\gamma = 1$, $\delta = 2$, and $\nu = 1$. This phase diagram exhibits a multicritical point at $\alpha = \beta = 0$; however, at this point *four* phases coexist.

which means that here a first-order transition to the disordered phase occurs.

A multicritical point at which the disordered phase coexists with both AB as well as with A_3B (but not with B_3A) would require a tricritical point on the AB -disordered line, i.e., $\alpha = \gamma = 0$ as well as on the A_3B -disordered line, $\alpha = \beta = 0$. Apart from the fact that this is one condition more than the number of available parameters, this is also inconsistent with the topology of the phase diagram: For $\gamma < 0$ the phase diagram looks as in Fig. 7 ($\gamma = -1$, $\delta = 2$, $\nu = 1$), i.e., two standard triple points occur at

$$\alpha_t = \frac{3\gamma^2}{16\nu}, \quad (4.6)$$

$$\beta_t = \pm \frac{9}{4} \gamma \sqrt{\frac{9\gamma + 6\delta}{2\nu}}. \quad (4.7)$$

When γ tends to zero, the two triple points move to $\alpha = \beta = 0$. For $\gamma > 0$ the phase diagram topology is qualitatively different. In this case, the AB phase can only be stable for $\alpha < 0$, as seen from Eq. (4.2), which can be further simplified by truncation of F_{AB} after the fourth order. Since, however, the transition to A_3B occurs already at positive α values, no direct transition from the disordered phase to AB is possible except for $\beta = 0$. Figure 8 shows this case ($\gamma = 1$, $\delta = 2$, $\nu = 1$). The transition line separating AB from A_3B or B_3A is of first-order and occurs at

$$\alpha = - \frac{(A^2 + 2A)\beta^2}{36(3\gamma + 2\delta)} \quad (4.8)$$

with

$$A = \frac{1}{\delta} (2\gamma + \sqrt{4\gamma^2 + 2\gamma\delta}). \quad (4.9)$$

The point $\alpha = \beta = 0$ is then a multicritical point (which occurs for *all* values of $\gamma > 0$), but at which not three but *all four* phases coexist. For symmetry reasons, such a point can only occur at vanishing field $H = 0$. In fact, it is nothing but the already well-known multicritical point in Shockley's BW phase diagram,¹ which, in reality, is supposed to appear for sufficiently strong ferromagnetic next-nearest-neighbor interactions.⁹ It should be noted that for $\gamma = 0$ the phase diagram looks the same, the only difference being that the transition line $AB \leftrightarrow A_3B/AB \leftrightarrow B_3A$ is now given by

$$\alpha = -\nu \left(\frac{3\delta}{2\nu} \right)^{2/3} \left(\frac{\beta}{6\delta} \right)^{8/3}. \quad (4.10)$$

In summary, we find that Landau theory permits only a multicritical point at which *four* phases coexist. Two multicritical points with three-phase coexistence could only occur for nonvanishing β values, but there the transition $A_3B \leftrightarrow$ disordered is always of first order, as seen from Eq. (4.5). Hence the hypothesis of a multicritical point in our system is only supported by some numerical evidence, but not by Landau theory arguments.

On the other hand, it is questionable if Landau theory is able to describe the phenomena in the present system at all. First, the transition line $AB \leftrightarrow$ disordered belongs to the universality class of the three-dimensional Heisenberg model with cubic anisotropy. For this system, Landau theory predicts a *second-order* transition. It is only the inclusion of fluctuations that leads to the prediction of a first-order transition.¹⁹ It is not at all obvious that one can include these effects consistently by simply requiring $\gamma < 0$, in particular when the A_3B phase is present as well. We therefore believe that a real understanding is impossible without a full renormalization-group analysis. Second, one should note that our Hamiltonian is marginal in the sense that for ferromagnetic next-nearest-neighbor coupling $J_{NNN} < 0$ the phases re-

main the same but are stable down to $T=0$, while for $J_{NNN} > 0$ new phases appear that are more complicated and that need a more refined order parameter than $\tilde{\psi}$. We expect that quite a lot could be learned by considering a three-dimensional phase diagram with J_{NNN} as third axis.

V. DISCUSSION

Our simulation has yielded the location of the triple point of the nearest-neighbor fcc Ising antiferromagnet much more accurately than previous studies. As discussed in Sec. III, there are numerical hints of possible multicritical behavior. However, our data are by far too inaccurate to answer this subtle question. A definitive resolution by numerical simulation would probably require by far more computer power than was available to us. Landau theory predicts a standard triple point, but this result should be taken with care. The system is therefore also a challenge for analytical renormalization-group theory.

ACKNOWLEDGMENT

We thank the computer center at the University of Kaiserslautern (RHRK) for generous allocation of Cray time.

-
- ¹W. Shockley, *J. Chem. Phys.* **6**, 130 (1938).
²K. Binder, in *Advances in Solid State Physics*, edited by P. Grosse (Vieweg, Braunschweig, 1986), Vol. 26, pp. 133–168.
³O. J. Heilmann, *J. Phys. A* **13**, 263 (1980).
⁴G. André *et al.*, *J. Phys. (Paris)* **40**, 479 (1979).
⁵J. Villain, R. Bidaux, J.-P. Carton, and R. Conte, *J. Phys. (Paris)* **41**, 1263 (1980).
⁶J. Slawny, *J. Stat. Phys.* **20**, 711 (1979).
⁷J. Slawny, in *Phase Transitions and Critical Phenomena*, edited by C. Domb and J. L. Lebowitz (Academic, London, 1987), Vol. 11, pp. 127–205.
⁸J. Bricmont and J. Slawny, *J. Stat. Phys.* **54**, 89 (1989).
⁹J. L. Lebowitz, M. K. Phani, and D. F. Styer, *J. Stat. Phys.* **38**, 413 (1985).
¹⁰N. S. Kurnakow, S. Zemczuzny, and M. Zasedatelev, *J. Inst. Metals* **15**, 305 (1916).
¹¹C. H. Johansson and J. O. Linde, *Ann. Phys.* **78**, 439 (1925).
¹²C. H. Johansson and J. O. Linde, *Ann. Phys.* **82**, 449 (1927).
¹³C. H. Johansson and J. O. Linde, *Ann. Phys.* **25**, 1 (1936).
¹⁴W. Selke, in *Alloy Phase Stability*, edited by G. M. Stocks and A. Gonis (Kluwer, Dordrecht, 1989), pp. 205–232.
¹⁵F. Ducastelle, *Order and Phase Stability in Alloys* (North-Holland, Amsterdam, 1991).
¹⁶A. Finel and F. Ducastelle, *Europhys. Lett.* **1**, 135 (1986); **1**, 543(E) (1986).
¹⁷R. Kikuchi, *Phys. Rev.* **81**, 998 (1951).
¹⁸R. Kikuchi, *J. Chem. Phys.* **60**, 1071 (1974).
¹⁹D. J. Wallace, *J. Phys. C* **6**, 1390 (1973).
²⁰E. Domany, Y. Shnidman, and D. Mukamel, *J. Phys. C* **15**, L495 (1982).
²¹M. Fukugita, H. Miro, M. Okawa, and A. Ukawa, *J. Stat. Phys.* **59**, 1397 (1990).
²²J. M. Sanchez, D. de Fontaine, and W. Teitler, *Phys. Rev. B* **26**, 1465 (1982).
²³U. Gahn, *Z. Metall.* **64**, 268 (1973).
²⁴R. Tetot, A. Finel, and F. Ducastelle, *J. Stat. Phys.* **61**, 121 (1990).
²⁵A. Finel, in *Alloy Phase Stability*, edited by G. M. Stocks and A. Gonis (Kluwer, Dordrecht, 1989), pp. 269–280.
²⁶K. Binder, *Phys. Rev. Lett.* **45**, 811 (1980).
²⁷K. Binder, *Z. Phys. B* **45**, 61 (1981).
²⁸K. Binder, J. L. Lebowitz, M. K. Phani, and M. H. Kalos, *Acta Metall.* **29**, 1655 (1981).
²⁹U. Gahn, *J. Phys. Chem. Solids* **43**, 977 (1982).
³⁰U. Gahn, *J. Phys. Chem. Solids* **47**, 1153 (1986).
³¹H. Ackermann, S. Crusius, and G. Inden, *Acta Metall.* **34**, 2311 (1986).
³²H. T. Diep, A. Ghazali, B. Bengel, and P. Lallemand, *Europhys. Lett.* **2**, 603 (1986).
³³W. Janke, in *Computer Simulation Studies in Condensed Matter Physics*, edited by D. P. Landau, K. K. Mon, and H.-B. Schüttler (Springer, Berlin, 1994), Vol. 7.
³⁴H. Müller-Krumbhaar and K. Binder, *J. Stat. Phys.* **8**, 1 (1973).
³⁵A. M. Ferrenberg, D. P. Landau, and K. Binder, *J. Stat. Phys.* **63**, 867 (1991).